

## Structure–Property Relationships of a Tetrapyrrolidinyl PNP–Lariat Ether and Its Complexes with Potassium, Sodium, and Silver Cations

Krystyna Brandt,<sup>†</sup> Piotr Seliger,<sup>\*,‡</sup> Andrzej Grzejdziak,<sup>‡,‡,‡</sup> Tadeusz J. Bartczak,<sup>§</sup>  
Rafat Kruszynski,<sup>§</sup> Dariusz Lach,<sup>†</sup> and Jerzy Silberring<sup>†,||</sup>

Institute of Polymer Chemistry, Polish Academy of Science, 41-800 Zabrze, Poland, Department of General and Inorganic Chemistry, University of Łódź, 90-136 Łódź, Poland, X-Ray Crystallography Laboratory, Institute of General and Ecological Chemistry, Technical University of Łódź, 90-924 Łódź, Poland, and Faculty of Chemistry and Regional Laboratory, Jagiellonian University, 30-060 Kraków, Poland

Received April 18, 2000

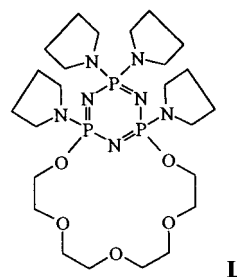
Spectral properties of the tetrapyrrolidinyl PNP–lariat ether, L, and its complexes with K<sup>+</sup>, Na<sup>+</sup>, and Ag<sup>+</sup> were investigated. Crystal structures of L and its complex with potassium iodide [KL]I were determined. Protonation constants of the ligand and formation constants of its complexes with Ag<sup>+</sup>, K<sup>+</sup>, and Na<sup>+</sup> in aqueous solutions were determined. <sup>1</sup>H NMR, <sup>31</sup>P NMR, FTIR, and ESIMS spectra as well as potentiometric measurements indicate that complexation of Ag<sup>+</sup> involves participation of the polyether oxygen donors and the endocyclic nitrogen atom of the cyclophosphazene ring. On the other hand, for complexation of K<sup>+</sup> and Na<sup>+</sup>, only polyether oxygen atoms are involved. The latter conclusion is confirmed in the solid-state structure of the [KL]I complex.

### Introduction

One of the most rapidly developing aspects in the research on new ligands is the design and synthesis of lariat ethers that are sidearmed crown ethers with the pendant group attached to the so-called pivot atoms (C, N, or P). The sidearms contain atoms with lone-pair electrons that may cooperate with those of heteroatoms in the macrocyclic polyether skeleton to provide a three-dimensional coordination of a ring-bound cation<sup>1</sup>.

Although many C- and N-pivot lariat ethers have been reported,<sup>1–4</sup> only a few P-pivot lariat ethers are known.<sup>5,6</sup> We have developed a new class of reactive crown ethers by incorporation of a chlorocyclophosphazene side-unit into the macrocyclic polyether skeleton.<sup>5,6</sup> By substitution of reactive chloride functions with various nucleophiles, in particular sodium arylates<sup>6–8</sup> and aliphatic amines,<sup>9–10</sup> we have obtained

a series of sidearmed PNP–crown derivatives that are P-pivot lariat ethers. From preliminary complexation studies by a simple chromatographic (TLC) test to the tetrapyrrolidinyl, cyclophosphazene PNP–crown derivative (L) has been selected as a promising PNP–lariat ether ligand that exhibits a wide spectrum of complexation abilities. Among the cations studied, K<sup>+</sup> and Ag<sup>+</sup> are the best complexed ones.<sup>11</sup> For L, there are three



L

structural units with the potential to take part in binding metal cations: (i) the polyether oxygen donors of the macrocyclic PNP–crown skeleton, (ii) the exocyclic nitrogen atoms of the pyrrolidinyl substituents (sidearms), and (iii) the endocyclic nitrogen atom of the cyclophosphazene ring. Cyclophosphazenes are known to display complexation ability, in particular, toward transition metal ions when strongly electron-donating substituents are linked to phosphorus atoms, which enhances the ring nitrogen basicity.<sup>12</sup>

K<sup>+</sup> and Ag<sup>+</sup> represent two different types of cations; hard potassium ion interacts electrostatically with oxygen and

\* To whom correspondence should be addressed.

<sup>†</sup> Polish Academy of Science.

<sup>‡</sup> University of Łódź.

<sup>§</sup> Technical University of Łódź.

<sup>||</sup> Jagiellonian University.

<sup>‡</sup> Deceased.

- (1) Gokel, G. W. *Chem. Soc. Rev.* **1992**, 39–47.
- (2) Katritzky, A. R.; Denisko, O. W.; Belyakov, S. A.; Schall, O. F.; Gokel, G. W. *J. Org. Chem.* **1996**, *61*, 7578–7584 and references therein.
- (3) Komiyama, M. *Prog. Polym. Sci.* **1993**, *18*, 871 and references therein.
- (4) Cacciapaglia, R.; Mandolini, L. *Chem. Soc. Rev.* **1993**, 221–232 and references therein.
- (5) Brandt, K.; Kupka, T.; Drozd, J.; van de Grampel, J. C.; Meetsma, A.; Jekel, A. P. *Inorg. Chim. Acta* **1995**, *228* (2), 187–192.
- (6) Brandt, K.; Porwolik, I.; Kupka, T.; Shaw, R. A.; Davies, D. B. *J. Org. Chem.* **1995**, *60*, 7433–7438.
- (7) Brandt, K.; Porwolik, I.; Olejnik, A.; Shaw, R. A.; Davies, D. B.; Hursthouse, M. B.; Sykara, G. D. *J. Am. Chem. Soc.* **1996**, *118*, 4496–4497.
- (8) Brandt, K.; Porwolik, I.; Siwy, M.; Kupka, T.; Shaw, R. A.; Davies, D. B.; Hursthouse, M. B.; Sykara, G. D. *J. Am. Chem. Soc.* **1997**, *119*, 12432–12440.
- (9) Brandt, K.; Porwolik, I.; Siwy, M.; Kupka, T.; Shaw, R. A.; Davies, D. B.; Hursthouse, M. B.; Sykara, G. D. *J. Am. Chem. Soc.* **1997**, *119*, 1143–1144.

- (10) Brandt, K.; Porwolik-Czomperlik, I.; Siwy, M.; Kupka, T.; Shaw, R. A.; Ture, S.; Clayton, A.; Davies, D. B.; Hursthouse, M. B.; Sykara, G. D. *J. Org. Chem.* **1999**, *64*, 7299–7304.
- (11) Brandt, K.; Porwolik-Czomperlik, I.; Siwy, M.; Kupka, T.; Shaw, R. A.; Davies, D. B.; Bartsch, R. A. *J. Inclusion Phenom. Macrocyclic Chem.* **1999**, *35*, 281–289.
- (12) Chandrasekhar, V.; Justin Thomas, K. R. *Appl. Organomet. Chem.* **1993**, *7*, 1–31 (review).

**Table 1.**  $^1\text{H}$  NMR Data for L and Its Complexes with  $\text{K}^+$ ,  $\text{Ag}^+$ , and  $\text{Na}^+$  Ions in  $\text{CDCl}_3$  and  $\text{D}_2\text{O}$ 

$^1\text{H}$ NMR, $\delta_{\text{H}}$ , ppm in $\text{CDCl}_3$									
	$\text{CH}_2\text{-C}$		$\text{CH}_2\text{N}$		$\text{CH}_2\text{O-C}$			$\text{CH}_2\text{O-P}$	
L (ligand)	1.763–1.754, m, 16H		3.123–3.103, m, 16H		3.766–3.60, m, 12H			4.038–3.971, m, 4H	
[KL]I	1.823–1.804, m, 16H <sup>a</sup>	2.999–2.988, m, 4H	3.182–3.087, m, 8H	3.234–3.192, m, 4H	3.562–3.505, m, 8H <sup>b</sup>	3.718–3.674, m, 4H <sup>b</sup>	3.839–3.803, m, 4H <sup>a</sup>	4.064–3.997, m, 2H	4.245–4.211, m, 2H <sup>a</sup>
[AgL]NO <sub>3</sub>	1.812–1.768, m, 16H		3.22–3.06, m, 16 H		3.44, s, 4H			3.760–3.558, m, 8H	
[NaL]I	1.776–1.769, m, 16H		3.125, m, 16H		3.646–3.604, m, 12H			3.735–3.698, m, 4H	
$^1\text{H}$ NMR, $\delta_{\text{H}}$ , ppm in $\text{D}_2\text{O}$									
	$\text{CH}_2\text{-C}$		$\text{CH}_2\text{N}$		$\text{CH}_2\text{O-C}$			$\text{CH}_2\text{O-P}$	
L (ligand)	1.735–1.666, m, 16H		2.995–2.966, m, 16H		3.667–3.54, m, 12H			3.938–3.888, m, 4H	
[KL]I	1.743–1.670, m, 16H <sup>a</sup>		2.990–2.972, m, 16H		3.674–3.519, m, 12H			3.878–3.867, m, 2H <sup>b</sup>	
[AgL]NO <sub>3</sub>	1.802–1.737, m, 16H <sup>a</sup>		3.174–3.104, m, 16 H <sup>a</sup>	3.84–3.76, m, 4H <sup>a</sup>	3.70–3.61, m, 8H <sup>a</sup>			4.10–4.02, m, 2H <sup>a</sup>	4.30–4.18, m, 2H <sup>a</sup>
[NaL]I	1.730–1.666, m, 16H		3.000–2.950, m, 16H		3.665–3.535, m, 8H			3.940–3.860, m, 4H	

<sup>a</sup> Broadening with a downfield shift relative to L. <sup>b</sup> Upfield shift relative to L.

nitrogen donor atoms, whereas silver cation forms mainly covalent bonds with the nitrogen atom.

According to the fundamental work by Shaw,<sup>13</sup> pyrrolidinylic cyclophosphazene derivatives are among the most basic so far observed. Therefore, incorporation of a pyrrolidinylic cyclophosphazene subunit into a crown ether structure might be expected to provide a polyheterotropic ligand with three different binding sites. The mode of complexation should be dependent on the type of complexed guest cation. Therefore, it was of interest to obtain complexes of ligand L with  $\text{K}^+$  and  $\text{Ag}^+$  and to probe the factors responsible for complexation by spectroscopic and electrochemical methods.

Furthermore, we sought to determine the X-ray crystal structures for L and its potassium complex. Solid-state studies, if not directly applicable to the solution phase, are very important in this area since they involve the key molecules (host and guest) and can confirm directly participation of the sidearm in cation binding.<sup>1</sup> For comparative purposes, electrochemical and spectroscopic studies of the complex of L with the size-complementary sodium cation have been also performed.

## Experimental Section

**Materials.** Ligand L was synthesized by the reported method.<sup>11</sup>

**(a) Synthesis of the Complex [KL]I.** Equimolar amounts of crystalline L (0.0609 g, 0.1 mmol) and KI (0.0166 g, 0.1 mmol) were dissolved in methanol (5 cm<sup>3</sup>) in an open vessel and allowed to evaporate, leaving colorless crystals. mp 160.3 °C; differential scanning calorimetry (DSC).

**(b) Synthesis of the Complex [NaL]I.** Equimolar amounts of crystalline L (0.040 g, 0.066 mmol) and NaI (0.010 g, 0.066 mmol) were dissolved in methanol (3 cm<sup>3</sup>) in an open vessel and allowed to evaporate, leaving a colorless viscous oil, which resisted any attempts to crystallize.

**(c) Synthesis of the Complex [AgL]NO<sub>3</sub>.** Equimolar amounts of crystalline L (0.0609 g, 0.1 mmol) and AgNO<sub>3</sub> (0.0170 g, 0.1 mmol) were dissolved in methanol (5 cm<sup>3</sup>) in an open vessel and allowed to evaporate, leaving a colorless viscous oil. Although the oil dissolved in organic solvents, it failed to crystallize. Spectral data for the ligand and the complexes are given in Tables 1 and 2.

**Methods.**  $^1\text{H}$  NMR spectra were recorded on a Varian VXR 300 spectrometer using solutions in  $\text{CDCl}_3$  (or in  $\text{D}_2\text{O}$ ) with tetramethylsilane (TMS) as internal reference.  $^{31}\text{P}$  NMR spectra were recorded on the same spectrometer operating at 121 MHz using solutions in  $\text{CDCl}_3$

**Table 2.**  $^{31}\text{P}$  NMR Data for L and Its Complexes with  $\text{K}^+$ ,  $\text{Ag}^+$ , and  $\text{Na}^+$  Ions in  $\text{CDCl}_3$  and  $\text{D}_2\text{O}$ 

$^{31}\text{P}$ NMR: A <sub>2</sub> B Spin System (in $\text{CDCl}_3$ )			
compound	$\delta P_A$ , ppm	$\delta P_B$ , ppm	$J_{P-P}$ , Hz
L	22.33	19.41	47.03
complex 1 ([KL]I)	21.85	19.71	48.73
complex 2 ([AgL]NO <sub>3</sub> )	21.05	18.61	45.21
complex 3 ([NaL]I)	22.33	19.41	46.92
$\Delta 1^a$	−0.48	+0.30	1.7
$\Delta 2^a$	−1.28	−0.80	−1.82
$\Delta 3^a$	0.00	0.00	−0.11
$^{31}\text{P}$ NMR: A <sub>2</sub> B Spin System (in $\text{D}_2\text{O}$ )			
compound	$\delta P_A$ , ppm	$\delta P_B$ , ppm	$J_{P-P}$ , Hz
L	21.76	19.79	41.99
complex 1 ([KL]I)	21.69	19.79	42.47
complex 2 ([AgL]NO <sub>3</sub> )	21.23	19.89	38.68
complex 3 ([NaL]I)	21.75	19.79	41.87
$\Delta 1^a$	−0.07	0.00	0.46
$\Delta 2^a$	−0.53	0.01	−3.11
$\Delta 3^a$	−0.01	0.00	−0.12

<sup>a</sup>  $\Delta(1, 2, 3)$ : differences in the chemical shift values for  $\delta P_A$  and  $\delta P_B$  and the  $^2J_{P-P}$  coupling constants between the respective complex (1, 2, or 3) and L.

or in  $\text{D}_2\text{O}$  and 85%  $\text{H}_3\text{PO}_4$  as an external reference with positive shifts recorded downfield from the reference. In most cases, both proton-coupled and proton-decoupled  $^{31}\text{P}$  NMR spectra were obtained.

Electrospray ionization mass spectrometric analysis (ESIMS) was performed with a Finnigan LCQ ion trap spectrometer (Finnigan, San Jose, CA). A solution of the sample was introduced into the ESIMS source by continuous infusion with the instrument's syringe pump at a rate of 3  $\mu\text{L}/\text{min}$ . The ESI source was operated at 4.25 kV, and the capillary heater was set to 200 °C. For fragmentation experiments, mass-selected monoisotopic molecular ions were isolated in the ion trap and collisionally activated with a 32% ejection radiofrequency amplitude at standard He pressure. The experiments were performed in the positive ion mode.

Liquid secondary ion mass spectrometry (LSIMS) was performed with an AMD 604 two-sector Intectra (Germany) mass spectrometer using glycerol and *m*-nitrobenzyl alcohol (NBA) matrixes. FTIR spectra were obtained with a Bio-Rad FTS-40A spectrometer with films deposited from chloroform solutions or KBr pellets. Melting points

**Table 3.** Crystal Data and Structure Refinement for L and [KL]I

	L	[KL]I
empirical formula	C <sub>24</sub> H <sub>48</sub> N <sub>7</sub> O <sub>5</sub> P <sub>3</sub>	C <sub>24</sub> H <sub>49</sub> IKN <sub>7</sub> O <sub>6</sub> P <sub>3</sub>
fw	607.60	790.61
cryst syst, space group	triclinic, <i>P</i> $\bar{1}$	triclinic, <i>P</i> $\bar{1}$
unit cell dimensions	<i>a</i> = 9.2510(10) Å <i>b</i> = 9.6780(10) Å <i>c</i> = 17.994(2) Å $\alpha$ = 83.730(10)° $\beta$ = 75.540(10)° $\gamma$ = 82.720(10)°	<i>a</i> = 9.5160(10) Å <i>b</i> = 13.7840(10) Å <i>c</i> = 14.0220(10) Å $\alpha$ = 91.320(10)° $\beta$ = 105.520(10)° $\gamma$ = 92.470(10)°
<i>V</i> , Å <sup>3</sup>	1542.4(3)	1769.4(3)
<i>Z</i>	2	2
calcd density, mg/m <sup>3</sup>	1.308	1.484
abs coeff, mm <sup>-1</sup>	2.147	9.830
final <i>R</i> indices	<i>R</i> 1 = 0.0807, [ <i>I</i> > 2σ( <i>I</i> )] w <i>R</i> 2 = 0.2307	<i>R</i> 1 = 0.0738, w <i>R</i> 2 = 0.1954
<i>R</i> indices (all data)	<i>R</i> 1 = 0.2190, w <i>R</i> 2 = 0.3305	<i>R</i> 1 = 0.1058, w <i>R</i> 2 = 0.2327

<sup>a</sup> Details in common: *T* = 293 K, λ(Cu Kα) = 1.54178 Å; refinement method, full-matrix least-squares on *F*<sup>2</sup>.

(detected as peaks on a curve) were determined on a DSC DuPont apparatus at a heating rate of 20 K/min using sealed aluminum pans (sample weight about 5 mg) in the air. pH-metric measurements were carried out with a RADELKIS OP-211/I pH meter and an OP-0808P combination electrode with an accuracy of ±0.01 pH unit. Potentiometric measurements were carried out with the use of a Meratronic V-543 multimeter and Ag<sup>0</sup>/0.01 M AgNO<sub>3</sub> + 0.1 M (C<sub>2</sub>H<sub>5</sub>)<sub>4</sub>NNO<sub>3</sub> in aqueous solution as the reference electrode.

**X-ray Crystal Structure of L and the Complex [KL]I.** Crystals of L and [KL]I were mounted on a KUMA-4 automatic four-circle diffractometer. The three-dimensional X-ray intensity data were collected with graphite monochromated Cu Kα radiation (λ = 1.54178 Å) at room temperature with the ω – 2θ scan modes. The unit cell parameters were determined from least-squares refinement of 99 reflections in the θ range of 5–60°. Details concerning the crystal data are given in Table 3.

Examination of three standard reflections monitored after each of the 97 reflections measured showed 69% loss of intensity. During data reduction, the decay correction coefficient was taken into account. The colorless crystal of L used for data collection became a brownish color. The three reference reflections of the crystal of [KL]I showed a 1.5% loss of intensity. Lorentz polarization and empirical absorption corrections for [KL]I were applied to the intensity data. The maximum and minimum transmission factors were 0.136 and 0.116, respectively, for [KL]I. The structures were solved by means of direct methods (L) and by the Patterson method ([KL]I). All non-hydrogen atoms were refined anisotropically using the full-matrix least-squares technique on *F*<sup>2</sup>. The hydrogen atom positions were partly located in the difference Fourier maps and partly set in calculated positions, treated as “riding” on the adjacent carbon atom [*d*(C–H) = 0.96 Å] and refined with an individual isotropic temperature factor equal to 1.2× the value of the equivalent temperature factor of the parent carbon atom. The solutions and refinements were performed with SHELXS97<sup>14</sup> and SHELXL97.<sup>15</sup> The graphical manipulations were performed using the XP routine of SHELXTL.<sup>16</sup> Atomic scattering factors were incorporated in the computer programs. Selected interatomic bond distances and angles are listed in Table 4.

## Results and Discussion

**NMR Measurements.** The <sup>1</sup>H NMR and <sup>31</sup>P NMR results for L and its complexes with K<sup>+</sup>, Na<sup>+</sup>, and Ag<sup>+</sup> are shown in

Tables 1 and 2. The <sup>1</sup>H NMR spectrum of the [KL]I complex indicates participation of both polyether oxygen and pyrrolidinyll nitrogen donors in the complexation of K<sup>+</sup>. Splitting of each CH<sub>2</sub>O–C and CH<sub>2</sub>N multiplet into three separate groups of peaks may be due to the lack of symmetry in the complex molecule, resulting from distortion from planarity of the N<sub>3</sub>P<sub>3</sub> ring (revealed by the X-ray crystallography), and the incorporation of one water molecule to the complex, which provides an additional oxygen donor for coordinative binding of K<sup>+</sup> (Figure 2).

In aqueous solution, there is a great possibility of competitive hydration of K<sup>+</sup> by the oxygen atoms of the solvent, and the effect of complexation on the <sup>1</sup>H NMR spectra is much less distinctive (Table 1). The only noticeable difference is splitting in two of the multiplets for the CH<sub>2</sub>O–P protons for [KL]I relative to L. That may indicate that only one of these two groups is involved in complexation, whereas two other oxygen atoms necessary for the most favorable hexacoordination of the potassium ion<sup>1,17</sup> are co-opted from the free water molecules.

In keeping with that hypothesis, no significant changes have been observed in the spectrum of the free ligand L on complexation with Na<sup>+</sup>, which is size-fit to the PNP cavity as the template used for the synthesis of the parent PNP–crown structure<sup>5</sup> that probably results in the nondistorted “nesting” conformation of the complex [NaL]I.

**<sup>1</sup>H NMR Spectrum of Complex [AgL]NO<sub>3</sub> in CDCl<sub>3</sub>.** As shown in Table 1, the CH<sub>2</sub>–C proton signals are significantly broadened and shifted downfield relative to those of the free ligand, with noticeable broadening of the multiplet corresponding to the CH<sub>2</sub>–N protons.

In the region for CH<sub>2</sub>O–C protons, which for L shows a barely discernible multiplet in the range of 3.76–3.60 ppm, the complexation involved separation of the multiplet into two parts of nearly equal intensity: a sharp singlet at 3.44 ppm (upfield shift) and a multiplet at 3.76–3.56 ppm, very close to that of the free ligand. Also, from the multiplet of the CH<sub>2</sub>O–P protons at 4.04–3.97 ppm, parts of the signals have been shifted downfield (to 4.15–4.10 ppm) as a result of complexation. This suggests some nonequivalence of the particular CH<sub>2</sub>O–C and CH<sub>2</sub>O–P groups because of the plausible distortion of the N<sub>3</sub>P<sub>3</sub> ring from the planarity found for the complexes of some donor-substituted cyclophosphazenes with transition metal cations.<sup>12</sup>

Comparison of the spectra for L and the complex [AgL]NO<sub>3</sub> taken in D<sub>2</sub>O and CDCl<sub>3</sub> shows a less distinctive effect from the solvent than in comparison of L and the [KL]I complex. Complexation resulted in an upfield shift of all groups of signals observed for L, particularly noticeable in the absorptions for CH<sub>2</sub>–N and CH<sub>2</sub>O–P protons, together with significant broadening of the respective multiplets. Peaks for the CH<sub>2</sub>O–C groups showed less splitting in the spectrum of [AgL]NO<sub>3</sub> taken in D<sub>2</sub>O than in CDCl<sub>3</sub>. Presumably, this is due to competitive ligation of Ag<sup>+</sup> by the D<sub>2</sub>O oxygen donors.

The <sup>31</sup>P spectra of the ligand and its complexes with Ag<sup>+</sup> and K<sup>+</sup> ions are both of the A<sub>2</sub>B type. They show a typical eight-line resonance pattern (with a line broadening at 1 Hz), which at higher frequency (5 Hz) collapses into a doublet and a triplet that are assigned to the two macrocyclic P atoms and the exomacrocyclic P atom, respectively (Table 2).

For the complex [KL]I in CDCl<sub>3</sub>, signals of the macrocyclic phosphorus atoms P<sub>A</sub> are shifted upfield as compared to those of the free ligand (22.33 for L→21.85 ppm for [KL]I), whereas for the exomacrocyclic dipyrrolidinyll-substituted P atoms, P<sub>B</sub>,

(14) Sheldrick, G. M. *SHELXS-97: Program for the Solution of Crystal Structures*; University of Göttingen: Göttingen, Germany, 1997.

(15) Sheldrick, G. M. *SHELXL-97: Program for the Solution and Refinement of Crystal Structures*; University of Göttingen: Göttingen, Germany, 1997.

(16) Sheldrick, G. M. *Release 4.1 of SHELXTL PC for Siemens Crystallographic Systems*; Siemens Analytical X-Ray Instruments Inc.: Madison, WI, 1990.

(17) Hancock, R. D. *Pure Appl. Chem.* **1986**, *58*, 1445.

**Table 4.** Selected Structural Data for the P<sub>3</sub>N<sub>3</sub> Rings in L and [KL]I (Distances in Å, Angles in Deg)

Phosphazene Ring Bond Lengths					
	L	[KL]I		L	[KL]I
P(1)–N(1)	1.531(5)	1.594(5)	P(2)–N(3)	1.582(4)	1.592(5)
P(1)–N(2)	1.582(6)	1.560(5)	P(3)–N(3)	1.589(5)	1.561(5)
P(2)–N(2)	1.587(6)	1.596(5)	P(3)–N(1)	1.583(6)	1.590(4)
Bond Lengths Exocyclic to the P <sub>3</sub> N <sub>3</sub> Ring					
	L	[KL]I		L	[KL]I
P(1)–O(1)	1.584(6)	1.596(4)	P(2)–N(6)	1.656(6)	1.642(5)
P(1)–N(4)	1.619(6)	1.627(5)	P(3)–N(7)	1.627(6)	1.626(5)
P(2)–N(5)	1.619(4)	1.634(6)	P(3)–O(5)	1.586(5)	1.600(4)
Bond Angles Within the P <sub>3</sub> N <sub>3</sub> Ring					
	L	[KL]I		L	[KL]I
N(1)–P(1)–N(2)	118.9(3)	116.0(2)	P(2)–N(3)–P(3)	122.3(4)	124.1(3)
P(1)–N(2)–P(2)	122.7(3)	122.8(3)	N(3)–P(3)–N(1)	116.8(3)	116.2(2)
N(2)–P(2)–N(3)	115.3(3)	114.9(2)	P(3)–N(1)–P(1)	121.6(4)	120.3(3)
Bond Angles Exocyclic to the P <sub>3</sub> N <sub>3</sub> Ring					
	L	[KL]I		L	[KL]I
O(1)–P(1)–N(1)	109.4(3)	103.8(2)	N(6)–P(2)–N(2)	106.6(3)	105.6(3)
O(1)–P(1)–N(4)	98.0(3)	102.1(2)	N(6)–P(2)–N(3)	114.8(3)	114.4(3)
O(1)–P(1)–N(2)	108.6(3)	112.1(3)	N(1)–P(3)–O(5)	109.0(3)	102.8(2)
N(4)–P(1)–N(2)	112.4(3)	108.9(3)	O(5)–P(3)–N(3)	109.2(3)	112.0(3)
N(4)–P(1)–N(1)	107.5(3)	113.0(3)	N(1)–P(3)–N(7)	109.7(4)	114.4(3)
N(5)–P(2)–N(6)	101.5(3)	103.0(3)	N(3)–P(3)–N(7)	109.0(3)	107.4(3)
N(5)–P(2)–N(2)	112.4(3)	114.7(3)	O(5)–P(3)–N(7)	102.0(3)	103.2(2)
N(5)–P(2)–N(3)	105.5(2)	103.8(3)			
Bond Lengths in 16-Membered Crown Ring					
	L	[KL]I		L	[KL]I
P(1)–O(1)	1.584(6)	1.596(4)	C(8)–O(5)	1.400(7)	1.430(6)
O(1)–C(1)	1.367(9)	1.450(7)	O(5)–P(3)	1.586(5)	1.600(4)
C(1)–C(2)	1.437(12)	1.478(9)	P(3)–N(1)	1.583(6)	1.590(4)
C(2)–O(2)	1.284(15)	1.417(7)	P(1)–N(1)	1.531(5)	1.594(5)
O(2)–C(3)	1.370(15)	1.400(8)	K(1)–O(1)		2.835(4)
C(3)–C(4)	1.432(15)	1.479(10)	K(1)–O(2)		2.917(4)
C(4)–O(3)	1.398(12)	1.409(8)	K(1)–O(3)		2.773(5)
O(3)–C(5)	1.391(12)	1.419(8)	K(1)–O(4)		2.894(4)
C(5)–C(6)	1.415(12)	1.468(11)	K(1)–O(5)		2.828(4)
C(6)–O(4)	1.435(11)	1.427(9)	K(1)–I(1)		3.550(1)
O(4)–C(7)	1.370(8)	1.432(9)	K(1)–O(66)		3.023(6)
C(7)–C(8)	1.411(9)	1.436(11)			
Torsion Angles					
	L	[KL]I		L	[KL]I
P(3)–N(1)–P(1)–O(1)	–135.6(4)	–95.0(3)	C(4)–O(3)–C(5)–C(6)	88(2)	–95.4(7)
N(1)–P(1)–O(1)–C(1)	80.3(8)	169.4(5)	O(3)–C(5)–C(6)–O(4)	66(2)	–65.5(7)
P(1)–O(1)–C(1)–C(2)	–118(1)	173.3(4)	C(5)–C(6)–O(4)–C(7)	–158(1)	174.9(5)
O(1)–C(1)–C(2)–O(2)	–60(2)	62.5(8)	C(6)–O(4)–C(7)–C(8)	167.8(9)	–172.4(6)
C(1)–C(2)–O(2)–C(3)	–142(2)	179.4(6)	O(4)–C(7)–C(8)–O(5)	–176.1(6)	60.3(9)
C(2)–O(2)–C(3)–C(4)	–94(2)	179.8(6)	C(7)–C(8)–O(5)–P(3)	122.1(7)	125.6(6)
O(2)–C(3)–C(4)–O(3)	96(2)	–68.4(8)	C(8)–O(5)–P(3)–N(1)	–64.5(7)	176.2(5)
C(3)–C(4)–O(3)–C(5)	–167(1)	167.0(7)	O(5)–P(3)–N(1)–P(1)	141.7(4)	104.9(3)

a slight downfield shift is observed. The coupling constant  $^2J_{P-P}$  for [KL]I is increased by 1.7 Hz as compared to L.

The observed changes may be due to the distortion of the N<sub>3</sub>P<sub>3</sub> ring from the planarity following the formation of the [KL]I complex. The upfield shift of the P<sub>A</sub> resonance signals might also result from an increase in the electronegativity of the polyether oxygen atoms taking part in the complexation of K<sup>+</sup> ion, which favors delocalization of the lone electron pairs of the N<sub>3</sub>P<sub>3</sub> ring nitrogens because of their shift toward the P<sub>A</sub> atoms.<sup>18</sup> Adjacent to the PNP macrocycle, pyrrolidinyl groups may contribute to that effect by shifting the lone electron pairs

of the pyrrolidinyl ring nitrogens toward the macrocyclic oxygens involved in coordination via P<sub>A</sub>-mediated intersubstituent electronic interactions, similar to those reported previously for aziridinylcyclophosphazenes bearing various O- or N-linked cosubstituents.<sup>19</sup>

However, the lack of any effect on the <sup>31</sup>P NMR spectra on complexation with size-complementary sodium cation excludes the latter hypothesis and supports the former hypothesis based on conformational changes of the ligand L involved by complexation. Despite the lack of unambiguous crystal data, it might be assumed that coordination of size-fit sodium cation, able to form a nesting complex with the ligand L, does not

(18) Allcock, H. R. *Phosphorus–Nitrogen Compounds: Cyclic, Linear and High Polymeric Systems*; Academic Press: New York, 1972.

(19) Brandt, K. *J. Mol. Struct.* **1991**, 243, 163.

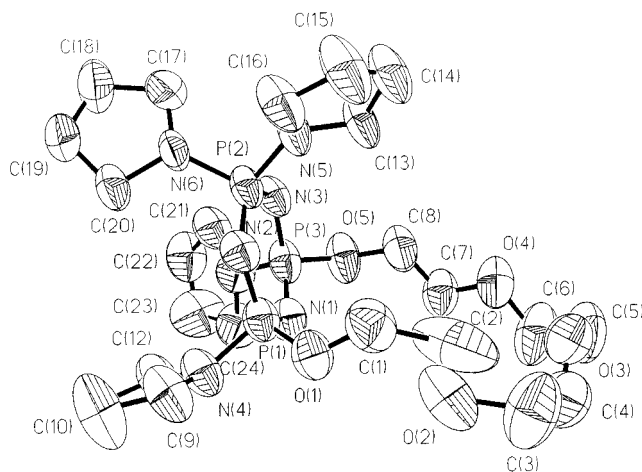


**Figure 1.** Perspective drawing of L showing the atom numbering. The thermal ellipsoids are plotted at 30% probability.

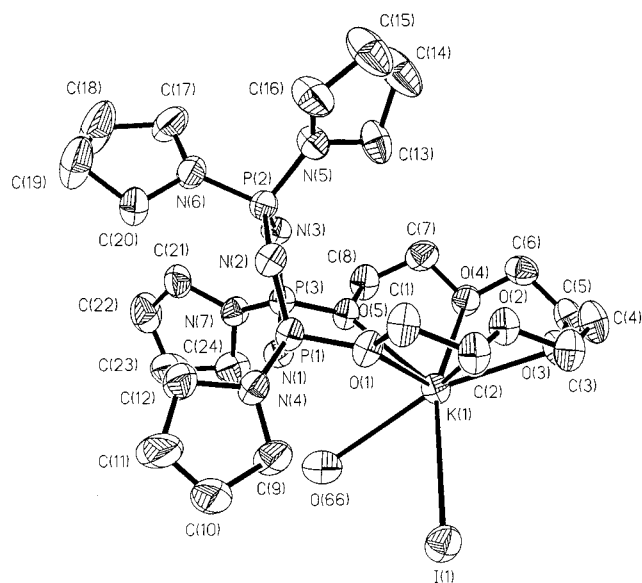


**Figure 2.** Perspective drawing of [KL]I showing the atom numbering. The thermal ellipsoids are plotted at 30% probability. Participation in the complexation of one additional nonmacrocylic oxygen atom, probably derived from a water molecule present in the sample of [KL]I, is observed, resulting in favorable hexacoordination of K<sup>+</sup>.

involve a distortion of the N<sub>3</sub>P<sub>3</sub> ring from planarity, as observed for the “perching” complex [KL]I with the “oversized” potassium ion (see Crystallographic Description of the Structures).

For complex [AgL]NO<sub>3</sub> in CDCl<sub>3</sub>, both signals of the macrocyclic phosphorus atoms, P<sub>A</sub>, and the exocyclic dipyrrolidinyl-substituted P atoms, P<sub>B</sub>, are shifted upfield, which indicates participation in the complexation of Ag<sup>+</sup> by at least one of the nitrogen atoms of the phosphazene ring (macrocylic nitrogen atom) as well as oxygen atoms and possibly the nitrogen donors of the side substituents. A contribution of N<sub>3</sub>P<sub>3</sub> ring nitrogen atoms in complexation of Ag<sup>+</sup> was first reported by Inoue et al.,<sup>20</sup> who have found an upfield shift of all P atoms of the cyclophosphazene ligand (polystyrene-bound ethoxycyclophosphazene) with a concomitant decrease in the <sup>2</sup>J<sub>P-P</sub> value. The latter is probably due to some ring distortion following complexation via the ring nitrogens. Similar decreases of the <sup>2</sup>J<sub>P-P</sub> value have been reported for complexes of (bis-pyrazolyl)cyclophosphazenes with W<sup>0</sup> and Mo<sup>0</sup> and have been

ascribed by Krishnamurthy et al. to deviation of the coordinating nitrogen atom from the plane of the other skeletal atoms.<sup>21</sup> Contrary to previous reports<sup>20,21</sup> for L, the predominant contribution to complexation is made by the donor atoms of the PNP-crown moiety, i.e., five polyether oxygens and the nitrogen atom from the -P=N-P= fragment of the N<sub>3</sub>P<sub>3</sub> ring incorporated into the crown-ether structure. Participation of only one of the three cyclophosphazene nitrogens in the ring is probably due to steric reasons that hinder involvement of the remaining two N<sub>3</sub>P<sub>3</sub> nitrogen atoms in coordination with Ag<sup>+</sup> immobilized inside the PNP-crown cavity. Therefore, changes in the <sup>31</sup>P NMR spectra in this case are less drastic than for the nonmacrocylic cyclophosphazene derivatives reported by Inoue's and Krishnamurthy's groups.<sup>21</sup>

As in the case of the <sup>1</sup>H NMR spectra in D<sub>2</sub>O, differences between the spectra of L and its complexes are less significant than those observed in CDCl<sub>3</sub>. This can also be explained by the effect of solvent, i.e., competitive coordination of the cations by the oxygens of D<sub>2</sub>O molecules.

**ESIMS and LSIMS Measurements.** The ESIMS spectrum of L revealed the presence of the molecular ion, at *m/e* 608, and a less abundant ion corresponding to the Na<sup>+</sup> adduct of the latter. ESIMS fragmentation analysis of L (Scheme 1, see Supporting Information) revealed two concurrent fragmentation patterns. One involves a stepwise loss of two pyrrolidinyl substituents, probably from the exomacrocylic P atom, and the other one involves a cleavage of the PNP-crown macrocycle and subsequent splitting-off of fragments of the polyether chain, followed by the stepwise loss of the pyrrolidinyl substituents initially adjacent to the PNP macrocycle.

LSIMS spectrum of [KL]I in the NBA matrix showed only the peak for the complex at *m/e* 646, while the ESIMS spectrum in methanol solution exhibited an intense peak for the 1:1 complex at *m/e* 646 and an additional weak peak at *m/e* 608 for the free ligand. When the ligand concentration was twice that of the potassium iodide, the ESIMS spectrum also showed another peak at *m/e* 1252, corresponding to a 1:2 sandwich complex.

Fragmentation of the molecular ion for the 1:1 complex (Scheme 2, see Supporting Information) showed an intense peak at *m/e* 506, corresponding to the loss of two pyrrolidinyl substituents (probably from the exomacrocylic P atom) and a less abundant peak at *m/e* 437, corresponding to the loss of three pyrrolidinyl groups from the parent molecule. The latter ion did not fragment further, suggesting possible involvement of one of the pyrrolidinyl groups proximal to the PNP macrocycle in the coordination of the crown-complexed K<sup>+</sup>. Quite a similar fragmentation pattern has been revealed for the complex [NaL]I (Scheme 2, see Supporting Information), confirming the same complexation mode for both of these alkali metal cations.

The LSIMS spectrum of an equimolar mixture of L and AgNO<sub>3</sub> shows a single peak at *m/e* 714 for a 1:1 complex. ESIMS spectral analysis of the same sample dissolved in methanol exhibits a molecular ion for the complex and a peak for the free ligand at *m/e* 608. Fragmentation of the molecular ion at *m/e* 714 shows stepwise splitting-off of two pyrrolidinyl substituents (*m/e* 640.9 and 571.8), probably from the exocyclic P atom, which is followed by stepwise splitting-off of the exomacrocylic fragment of the cyclophosphazene ring with pyrrolidinyl groups (Scheme 3, see Supporting Information).

Decomposition of the N<sub>3</sub>P<sub>3</sub> ring begins with a loss of the substituent-deprived P-N unit, yielding the fragmentation ion

(20) Inoue, K.; Ooshita, Y.; Itaya, T.; Nakamura, H. *Macromol. Chem. Phys.* **1997**, *98*, 3173–3184.

(21) Chandrasekaran, A.; Krishnamurthy, S. S.; Nethaji, M. *J. Chem. Soc., Dalton Trans.* **1994**, 63–68.

at  $m/e = 535$  (the most intense peak, probably due to a strong resonance stabilization). Next, the second ring nitrogen with the adjacent pyrrolidinyl group is split off, yielding the  $\text{Ag}^+$  conjugate of the monopyrrolidinyl PNP–crown fragment and finally converts into  $\text{Ag}^+$  complexed by the substituent-free PNP–macrocyclic moiety,  $m/e = 378$  (Scheme 3, see Supporting Information).

As was the case for  $\text{K}^+$  complex formation with L, the ESIMS spectra of the  $\text{Ag}^+$  complex obtained when the L concentration is twice that of the  $\text{AgNO}_3$  in methanol solution shows a peak at  $m/e = 1323$  corresponding to a 1:2 sandwich complex. Conversely, no sandwich formation was revealed in the ESIMS spectra of the mixtures of L with NaI, irrespective of the molar ratio of the components.

**FTIR Spectra.** Comparison of the FTIR spectra of L and the [KL]I complex reveals the most significant changes in the region of  $1000\text{--}1150\text{ cm}^{-1}$ , corresponding to the stretching vibrations of P–O–C and the P–N–C bonds, and in the region of  $1290\text{--}1460\text{ cm}^{-1}$ , characteristic of the stretching vibrations of the N–C bonds in the pyrrolidinyl substituents. The latter change is particularly dramatic: two separate, low intensity bands at  $1348$  and  $1456\text{ cm}^{-1}$  for the free ligand (probably corresponding to the pyrrolidinyl groups linked to the remote P atom and adjacent to the PNP macrocycle, respectively), collapse into one, slightly split, intense band with maxima at  $1352$  and  $1377\text{ cm}^{-1}$ . This might support the hypothesis about the intersubstituent electronic interactions involved by the coordination of  $\text{K}^+$  ions by oxygen donors.<sup>19</sup> Some contribution to the above spectral changes from hydrogen bonding with the incorporated complex structure water molecule (see Figure 2) cannot also be excluded. (The latter presumption might be supported by the fact that almost no change in this region is observed for the complex of the ligand L with the sodium cation size-fit to the PNP–crown cavity.)<sup>5</sup> On the other hand, there is almost no change in the absorption for the  $\text{N}_3\text{P}_3$  ring after complexation ( $1201\text{ cm}^{-1}$  for L and  $1199\text{ cm}^{-1}$  for [KL]I). This excludes any appreciable participation of the  $\text{N}_3\text{P}_3$  ring nitrogen atoms in the coordination of  $\text{K}^+$ .

Comparison of the IR spectra of L and its complex with  $\text{Ag}^+$  shows broadening of the absorption band at  $990\text{--}1170\text{ cm}^{-1}$ , characteristic for P–O–C and C–O–C bonds, and a shift of the band at  $1201\text{ cm}^{-1}$  in L, which is characteristic of the stretching vibrations of the P–N=P bonds of the  $\text{N}_3\text{P}_3$  ring to  $1226\text{ cm}^{-1}$  in the complex. The spectacular shift of the P–N band indicates an involvement of at least one endocyclic ring nitrogen atom in complexation with  $\text{Ag}^+$  that is consistent with the results of the  $^{31}\text{P}$  NMR investigations described earlier. The differences between the FTIR spectra of the free ligand and its  $\text{Ag}^+$  complex observed in the region of  $750\text{--}1000\text{ cm}^{-1}$  may be ascribed to conformational changes within the polyether macrocycle, which are known to accompany its involvement in complexation with various metal cations. Detailed IR spectroscopic studies of conformational changes following complexation of alkali and alkali earth metal cations by crown ethers and benzo–crown ethers have been reported.<sup>22,23</sup>

The DSC curve for a crystalline sample of [KL]I showed three maxima of endothermic effects: at  $64\text{ }^\circ\text{C}$ ,  $\Delta H = 118\text{ J/g}$  (due to loss of methanol that had been incorporated when the complex was crystallized and evident in the  $^1\text{H}$  NMR spectrum of the crystalline complex); at  $123.9\text{ }^\circ\text{C}$ ,  $\Delta H = 4.26\text{ J/g}$  (probably due to loss of the water molecule from the parent

complex); and at  $160.3\text{ }^\circ\text{C}$ ,  $\Delta H = 153.5\text{ J/g}$ . Free L exhibited a melting point at  $109.2\text{ }^\circ\text{C}$  ( $\Delta H = 28.3\text{ J/g}$ ), preceded by an endothermic minimum at  $52.7\text{ }^\circ\text{C}$  ( $\Delta H = 11.2\text{ J/g}$ ); the latter was probably due to a loss of hexane from the clathrate that was formed during crystallization from this solvent.

**Crystallographic Description of the Structures. Structure of L.** A perspective view of each of the structures together with their atom numbering scheme is shown in Figures 1 (L) and 2 ([KL]I). The molecule L can be considered a hybrid compound consisting of two condensed entities: (i) an inorganic cyclophosphazene ring,  $\text{N}_3\text{P}_3$ , substituted by four pyrrolidinyl rings at the P atoms; and (ii) a 16-membered PNP–crown macrocycle, sharing the atoms P(1), N(1), and P(3). The 16-membered ring adopts a distorted crown conformation and can be divided into two parts. One is a relatively stiff part consisting of the O(1)–P(1)–N(1)–P(3)–O(5) fragment that acts as an anchor because of the steric constraints imposed by the geometry of the  $\text{N}_3\text{P}_3$  ring. The remaining part is rather flexible and shows some signs of disorder in the region of the –C(2)–O(2)–C(3)– atoms. This part of the molecule exhibits rather large thermal motion (Figure 1), which affects the bond lengths C(2)–O(2) =  $1.284(15)\text{ \AA}$  and O(2)–C(3) =  $1.370(15)\text{ \AA}$ . Also, the pyrrolidine ring N(5)–C(13)–C(14)–C(15)–C(16) shows some disorder. The cyclophosphazene ring is distorted from planarity. The largest deviation from the least-squares plane through P(1), N(2), P(2), N(3), P(3), and N(1) is  $-0.099(2)\text{ \AA}$  for P(3). All but one endocyclic P–N bond length are equal within experimental error with a mean value of  $1.585(5)\text{ \AA}$ . Significantly shorter is the P(1)–N(1) bond at  $1.531(5)\text{ \AA}$ . The average exocyclic P–N bond length is  $1.630(6)\text{ \AA}$ . The cyclophosphazene ring makes a  $72.8(1)^\circ$  angle with the “crown” ring plane defined by atoms O(1), O(2), O(3), O(4), and O(5). The 5-membered pyrrolidine rings form angles with the  $\text{P}_3\text{N}_3$  ring of  $81.7(4)$ ,  $72.0(3)$ ,  $72.0(2)$ , and  $51.0(3)^\circ$  for the N(4), N(5), N(6), and N(7) rings, respectively.

**Structure of [KL]I.** The  $\text{P}_3\text{N}_3$  cyclophosphazene ring in the complex is even more severely distorted from planarity than it was in L. Two endocyclic P–N distances are significantly shorter than the average of  $1.593(5)\text{ \AA}$ , i.e., P(1)–N(2) =  $1.560(5)\text{ \AA}$  and P(3)–N(3) =  $1.561(5)\text{ \AA}$ . The cyclophosphazene ring is folded along a line joining P(1) and P(3). Deviations of atoms from the plane defined by P(3), N(1), and P(1) are  $0.67(1)$ ,  $0.91(1)$ , and  $0.43(1)\text{ \AA}$  for N(2), P(2), and N(3), respectively. This plane forms an angle of  $18.2^\circ$  with the plane defined by all six atoms. Insertion of  $\text{K}^+$  ion into the crown stabilizes the structure and reduces the thermal movement of atoms (Figures 1 and 2). The mean K–O distance is  $2.849(4)\text{ \AA}$ . The  $\text{K}^+$  deviates by  $1.328(2)\text{ \AA}$  from the least-squares plane defined by the O(1), O(2), O(3), O(4), and O(5) atoms. The K–I bond length is  $3.550(1)\text{ \AA}$ . At the end of refinement, a maximum of approximate height  $4e\text{ \AA}^{-3}$  appeared in a difference Fourier synthesis and was interpreted as an OH group, O(66). The possibility of the N(1) atom coordinating to  $\text{K}^+$  is excluded on the basis of a large K–N(1) bond distance of  $3.467(5)\text{ \AA}$ .

**Potentiometric Measurements. (a) Protonation Constants of L.** Investigated ligand L, because of the presence of the four pyrrolidinyl groups, shows basic properties and relatively good solubility in water. This made it possible to determine the protonation constants of this compound. The values were determined by the classical pH-metric method. Solutions containing  $c\text{L} + 5c\text{HNO}_3$  ( $c = 10^{-3}\text{--}10^{-2}\text{ M}$ ) with an ionic strength  $\mu = 0.1$  ( $(\text{C}_2\text{H}_5)_4\text{NNO}_3$ ) were titrated by  $(\text{C}_2\text{H}_5)_4\text{NOH}$ . Values of the protonation constants were calculated using

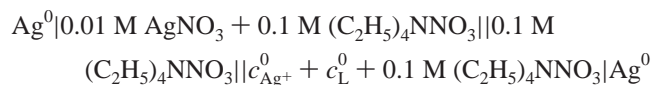
(22) Trofimov, V. A.; Kireeva, I. K.; Generalova, I. B.; Tsvadze, A. I. *Russ. J. Coord. Chem.* **1990**, *16*, 1459–1474.

(23) Raevskij, A. O. *Russ. J. Coord. Chem.* **1990**, *16*, 723–746.

programs based on the algorithms PKAS<sup>24</sup> and MINIGLASS ( $\log K_1 = 5.70 \pm 0.02$ ,  $\log K_2 = 1.91 \pm 0.1$ ,  $\log K_3 < 1$ ,  $\log K_4 \ll 1$ ).<sup>25</sup>

**(b) Determination of the Complex Formation Constants.**

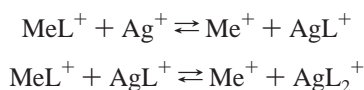
Formation constants of  $\text{Ag}^+$  complexes with L in water were determined by simple titration of the ligand with a  $\text{AgNO}_3$  solution and measurement of the electromotive force (emf) in the system:



where  $c_{\text{Ag}^+}^0 = 10^{-2} - 10^{-1} \text{ M}$  and  $c_{\text{L}}^0 = 10^{-3} - 10^{-2} \text{ M}$ .

The activity of the uncomplexed silver ions was calculated from the emf values using the Nernst equation. The constants were calculated numerically as previously reported<sup>26</sup> to be  $\log \beta_{01} = 3.26 \pm 0.02$  and  $\log \beta_{12} = 2.30 \pm 0.02$ .

The complex formation constants for  $\text{K}^+$  and  $\text{Na}^+$  were determined using the same system and procedure, but before titration, a precise amount of  $\text{KNO}_3$  or  $\text{NaNO}_3$ , respectively, was added to the ligand solution. During the titration, the following equilibria were established:



where  $\text{Me}^+ = \text{K}^+$  or  $\text{Na}^+$ .

Knowing the formation constants of the silver complexes with L and the concentrations of the uncomplexed silver ions, all other concentrations are available, and the stability constants for  $\text{K}^+$  and  $\text{Na}^+$  complexes were calculated. A similar method was used to determine the formation constants of  $\text{Pb}^{2+}$ ,  $\text{Tl}^+$ , and  $\text{K}^+$  complexes with cryptands in nonaqueous solutions<sup>27,28</sup> as well as lanthanide ion complexes with crown ethers in propylene carbonate.<sup>29</sup> The obtained values were  $\log \beta_{01} = 1.02 \pm 0.05$  and  $\log \beta_{01} = 1.20 \pm 0.05$  for  $\text{K}^+$  and  $\text{Na}^+$ , respectively.

Comparison of the formation constant values (in water) for  $\text{K}^+$  complexes with crown ethers (15C5,  $\log \beta = 0.74 - 0.76$ <sup>30,31</sup> and 18C6,  $\log \beta = 2.04 - 2.06$ )<sup>30,32</sup> and for  $\text{Na}^+$  complexes (15C5,  $\log \beta = 0.67 - 0.79$ <sup>30,31,33,34</sup> and 18C6,  $\log \beta = 0.80 -$

$0.82$ )<sup>30,33,35</sup> with those obtained for our complexes indicates a similar mode of complexation.

Because of the presence of the PNP heterounit in the polyether macrocyclic ring, L should have a larger bonding cavity than 15C5 (0.86–0.92 Å), which should result in a better size-fit of L with  $\text{Na}^+$  (radius = 1.02 Å). This cation/cavity complementarity makes the electrostatic repulsion much higher and causes the increase of the complex  $[\text{NaL}]^+$  stability to the value of  $\log \beta = 1.20$ . Similar rationale seems plausible for the established enhancement of the formation constant value for  $[\text{KL}]^+$  with respect to that for the complex  $\text{K}[15\text{C5}]^+$ .

Comparison of the formation constants of  $\text{Ag}^+$  complexes in  $\text{H}_2\text{O}$  for the crowns 15C5 ( $\log \beta = 0.94$ )<sup>30</sup> and 18C6 ( $\log \beta = 1.51 - 1.60$ )<sup>32,36</sup> with that obtained for our ligand ( $\log \beta_{02} = 5.56$ ) reveals a different mode of  $\text{Ag}^+$  coordination. The higher stability constant for the  $[\text{AgL}]^+$  complex in comparison to the crown-ether complexes of  $\text{Ag}^+$  and alkali metal ions is attributed to the presence in the macrocyclic ring of a nitrogen donor atom known to form a strong, highly covalent bond with soft  $\text{Ag}^+$ . A similar effect was observed by Frensdorf<sup>36</sup> in the case of replacement of oxygen by nitrogen in 18-membered macrocyclic multidentate ligands. Participation of the nitrogen atom of the phosphazene ring in the  $\text{Ag}^+$  coordination process is confirmed by the <sup>31</sup>P NMR and FTIR spectra presented earlier in this paper. The radius of the  $\text{Ag}^+$  ( $r = 1.15 \text{ \AA}$ )<sup>37</sup> is bigger than the radius of the bonding cavity of the investigated ligand, hence there is the possibility for formation of relatively stable sandwich complexes ( $[\text{AgL}_2]^+$ ) in the aqueous as well as in the methanol solutions employed for the ESIMS measurements.

**Acknowledgment.** This work was supported by the Polish Research Council (KBN Grants 3 T09A 001 13 and 3 T09A 140 15) and the Maria Skłodowska-Curie Fund II (Grant PAN/NSF-97-307).

**Supporting Information Available:** Two X-ray crystallographic files in CIF format for ligand L and for complex  $[\text{KL}]$ . Schemes 1–3 showing the results of ESI fragmentation analysis for the molecular ions derived from the free ligand and its complexes with K, Na, and Ag cations. This material is available free of charge via the Internet at <http://pubs.acs.org>.

IC000430Q

- (24) Motekajtis, R. J.; Martel, A. E. *Can. J. Chem.* **1992**, *60*, 168–173.  
 (25) Izquierdo, A.; Beltran, J. L. *Anal. Chim. Acta* **1986**, *181*, 87–96.  
 (26) Ignaczak, M.; Grzejdzak, A.; Andrijewski, G. *Russ. J. Electrochem.* **1991**, *27*, 904–910.  
 (27) Gutknecht, J.; Schneider, H.; Stroka, J. *Inorg. Chem.* **1978**, *17*, 3326–3329.  
 (28) Cox, B. G.; Garcia-Rosas, J.; Schneider, H.; van Truong, Ng. *Inorg. Chem.* **1986**, *25*, 1168–1168.  
 (29) Bunzli, J. C. G.; Pilloud, F. *Inorg. Chem.* **1989**, *28*, 2638–2642.

- (30) Izatt, R. M.; Terry, R. E.; Haymore, B. L.; Hansen, L. D.; Dalley, N. K.; Avondet, A. G.; Christensen, J. J. *J. Am. Chem. Soc.* **1976**, *98*, 7620–7626.  
 (31) Cygan, A.; Biernat, J. F.; Chadzynski, H. *Pol. J. Chem.* **1979**, *53*, 929–933.  
 (32) Christensen, J. J.; Eatough, D. J.; Izatt, R. M. *Chem. Rev.* **1974**, *74*, 351–384.  
 (33) Hoiland, H.; Ringseth, J. A.; Brun, T. S. *J. Solution Chem.* **1979**, *8*, 779–791.  
 (34) Dishong, D. M.; Gokel, G. W. *J. Org. Chem.* **1982**, *47*, 147–148.  
 (35) Lin, J. D.; Popov, A. I. *J. Am. Chem. Soc.* **1981**, *103*, 3773–3777.  
 (36) Frensdorf, H. K. *J. Am. Chem. Soc.* **1971**, *93*, 600–606.  
 (37) Izatt, R. M.; Bradshaw, J. S.; Nielsen, S. A.; Lamb, J. D.; Christensen, J. J. *Chem. Rev.* **1985**, *85*, 271–339.